

See discussions, stats, and author profiles for this publication at: <https://www.researchgate.net/publication/248703583>

High Fluorescence of Thioflavin T Confined in Mesoporous Silica Xerogels

ARTICLE *in* LANGMUIR · JULY 2013

Impact Factor: 4.46 · DOI: 10.1021/la402406g · Source: PubMed

CITATIONS

7

READS

26

7 AUTHORS, INCLUDING:



Giorgio Schirò

French National Centre for Scientific Research

33 PUBLICATIONS 372 CITATIONS

SEE PROFILE



Maurizio Leone

Università degli Studi di Palermo

154 PUBLICATIONS 2,409 CITATIONS

SEE PROFILE



Valeria Militello

Università degli Studi di Palermo

62 PUBLICATIONS 1,059 CITATIONS

SEE PROFILE



Valeria Vetri

Università degli Studi di Palermo

39 PUBLICATIONS 768 CITATIONS

SEE PROFILE

High Fluorescence of Thioflavin T Confined in Mesoporous Silica Xerogels

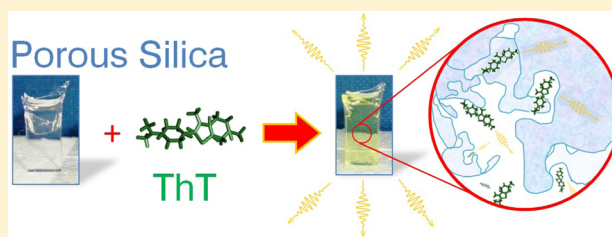
Michele D'Amico,^{*,†} Giorgio Schirò,^{†,‡} Antonio Cupane,[†] Laura D'Alfonso,[§] Maurizio Leone,[†] Valeria Militello,[†] and Valeria Vetri[†]

[†]Dipartimento di Fisica e Chimica, Università degli Studi di Palermo, Via Archirafi 36, I-90123 Palermo, Italy

[§]Dipartimento di Fisica G. Occhialini, Università degli Studi di Milano-Bicocca, Piazza della Scienza 3, I-20126 Milano, Italy

ABSTRACT: Trapping of organic molecules and dyes within nanoporous matrices is of great interest for the potential creation of new materials with tailored features and, thus, different possible applications ranging from nanomedicine to material science. The understanding of the physical basis of entrapment and the spectral properties of the guest molecules within the host matrix is an essential prerequisite for the design and control of the properties of these materials. In this work, we show that a mesoporous silica xerogel can efficiently trap the dye thioflavin T

(ThT, a molecule used as a marker of amyloid fibrils and with potential drug benefits), sequestering it from an aqueous solution and producing a highly fluorescent material with a ThT quantum yield 1500 times greater than that of the free molecule. The study of spectroscopical properties of this system and the comparison with fluorescence of an uncharged analogue of ThT give indications about the mechanism responsible for the fluorescence switching-on of ThT molecules during their uptake into the glass. Diffusion and nanocapillarity are responsible for ThT absorption, whereas electrostatic interaction between positive ThT molecules and negative dangling $\equiv\text{SiO}$ groups covering the pore surfaces causes the immobilization of ThT molecules inside the pores and the enhancement of its fluorescence, in line with the molecular rotor model proposed for this dye. We also show that entrapment efficiency and kinetics can be tuned by varying the electrostatic properties of the dye and/or the matrix.



INTRODUCTION

In the last few years, the physical properties of small molecules confined in nanometric environments have been intensively investigated for both the sake of pure science and potential technological applications.^{1–7} From the viewpoint of applications, the possibility of tailoring the physical properties of molecules embedded in a porous system is really appealing for the creation of tunable lasers, sensors (pH sensors, food analysis sensors, environmental biosensors, and single-molecule sensors), drug-delivery systems, luminescent solar concentrators, molecular sieves, and other smart materials.^{1,2,4–6,8–10}

One of the methods to obtain a mesoporous material (i.e., with pore dimension in the range of 2–50 nm) is the sol–gel technique for the production of silica xerogel. Starting from a room-temperature mixture of water, acid, and a metal alkoxide precursor, it is possible to obtain a porous solid (xerogel).^{1,9,11–13} The as-obtained material is initially “wet”, and it progressively dries, losing its water content with a concomitant general matrix rearrangement that causes a marked ($\sim 1/8$ in volume) dimension reduction.^{9,13,14} “Dry” xerogels with hydration $h \sim 0.35$ (grams of $[\text{H}_2\text{O}]/\text{grams of } [\text{SiO}_2]$) are obtained after about 3 months of drying at room temperature.^{15,16}

The co-encapsulation of organic dye molecules into these materials is also used as a probe of the xerogel chemical structure and to follow its temporal modifications.^{1,8,9} Physical confinement of the molecules was studied by single-molecule

techniques probing the mobility of fluorescent dyes in xerogel materials and indicating in steric effect, ionic interactions, hydrogen-bonding interactions, and hydrophobic interactions the possible non-covalent molecule–matrix interactions.¹⁷ Moreover, the encapsulation of small molecules into silica matrices was realized to be a really promising approach because of the excellent sealing ability of silica and its high transparency and high compatibility with other materials.^{3,13} Beside its demonstrated biocompatibility, key advantages of these materials are their low cost and the relative simplicity of preparation and modification.^{3,4,11}

Thioflavin T (ThT) is a widely used organic molecule, which shows a switching-on of its light-blue fluorescence when it is found in a confining environment.¹⁸ Indeed, as it is well-assessed, the fluorescence signal of ThT in aqueous solution is almost vanishing for the presence of highly efficient internal non-radiative channels, while the fluorescence intensity shows a dramatic increase of 3 orders of magnitude in the presence of amyloid fibrils^{19–22} and in the presence of other different confining systems, from DNA to porous silicon.¹⁸

ThT recently also gained a renewed attention because it demonstrates high potential for medical application in aging processes.^{23,24} It was also intriguingly suggested that the

Received: February 28, 2013

Published: July 11, 2013

presence of ThT may affect the amount or size of proteins and peptides prone to aggregate or to form amyloid fibrils.^{23,25}

The recently proposed molecular model explaining the photophysics of the ThT molecule describes it as formed by two main planar parts constituted by the benzothiazole moiety and the dimethylanilino rings (see the structure shown in Figure 1), which can rotate each other around a single C–C

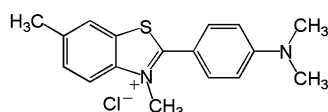


Figure 1. Chemical structure of ThT.

bond, forming an angle ϕ that varies from 37° in the ground electronic state [the two moieties of ThT form this angle $\phi = 37^\circ$ for the energetic compromise between the coplanar conformer ($\phi = 0^\circ$, favored by the “electronic effects” of its aromatic rings) and the steric disturbance of the methyl group] to 90° in the local photoexcited (LE) state.^{18,26–28} At this ϕ value, the LE state crosses a non-radiative twisted internal charge-transfer (TICT) state, which de-excites the molecule without photoemission (quantum yield of 10^{-4}).^{18,27,29} When the free rotations of ThT molecules are hindered, the ϕ angle cannot change and the LE state is not linked to the TICT state. In this case, the relaxation comes directly from the LE state by photon emission with a higher quantum yield. The fluorescence intensity controlled by the dihedral angle ϕ is what defines ThT as a molecular rotor.^{26,27,18}

ThT is a positively charged molecule because of the formal positive charge in the nitrogen atom of the benzothiazole group (see Figure 1). The negative counterion is a chlorine atom, which is completely dissociated from ThT in solution conditions.

In this work, we study the uptake of ThT in a silica xerogel via impregnation in an aqueous solution containing the dye and characterize the spectroscopic properties of the trapped dye molecules. The aim of this work is to gain information about the physical mechanisms responsible for the diffusion and trapping of the molecule in the host matrix and, at the same time, to characterize the resulting fluorescent glass. Indeed, we believe that the comprehension of the underlying physical

mechanisms is an essential requisite to “tune” the trapping of fluorescent molecules in such materials by regulating external conditions. Our results indicate that the used xerogels can irreversibly trap the ThT molecules sequestering them from the solution and giving a great enhancement of the dye fluorescence. Measurements of the uptake kinetics, of the ThT mobility inside the porous matrix, and of the static and time-resolved spectroscopic features of the trapped molecules and a comparison both with an uncharged analogue of ThT and with the uptake process performed in acidic conditions allow us to put forward a molecular model in which diffusion and nanocapillary forces are responsible for dye uptake, while the electrostatic interactions between the negative $\equiv\text{SiO}^-$ groups of the matrix and the positive ThT molecules play the key role in the entrapment. This offers the possibility to control the trapping efficiency and kinetics by modulating the electrostatic properties of the dye and/or the hosting matrix.

RESULTS AND DISCUSSION

The seminal observation of the present study is pictorially reported in the Table of Contents graphic: If a transparent, non-fluorescent, aged silica xerogel (density of $\sim 1.7 \text{ g/cm}^3$, indicating a highly porous matrix, with a hydration level of ~ 0.35) is dipped into a non-fluorescent water solution containing $\sim 40 \text{ }\mu\text{M}$ ThT, an intense fluorescence signal develops; at the same time, the ThT concentration in solution decreases. ThT molecules are trapped inside the xerogel with a final concentration higher than in the solution, and thus, the uptake is not just a diffusive process. Moreover, after a ThT-loaded xerogel is placed in a “clean” water solution for 48 h, bleaching of the sample yellowish green color or any presence of leached ThT into the solution was not observed, indicating that the loading process is irreversible at neutral pH.

The fluorescence of the entire system formed by the empty xerogel and the ThT solution (see the schematic representation in Figure 2a) was measured under excitation at 450 nm as a function of time during the ThT-uploading experiment. The spectrum at $t = 0$ (purple points in Figure 2a) does not show any significant ThT fluorescence band according to the very low quantum yield of ThT aqueous solution (it was also verified that the xerogel sample alone, excited at 450 nm, does not produce any fluorescence signal).²² Then, the strong

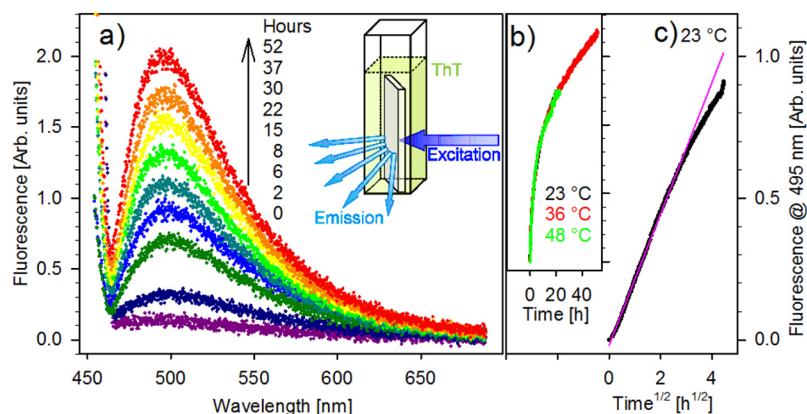


Figure 2. (a) Fluorescence spectra as a function of the uptake time at 36°C and the schematic representation of the experimental setup. (b) ThT fluorescence signal at 495 nm as a function of the uptake time for three temperatures: 23°C (black), 36°C (red), and 48°C (green). (c) ThT fluorescence signal at 495 nm (black) as a function of the square root of the uptake time at 23°C and the corresponding linear fit (purple) of the first hours.

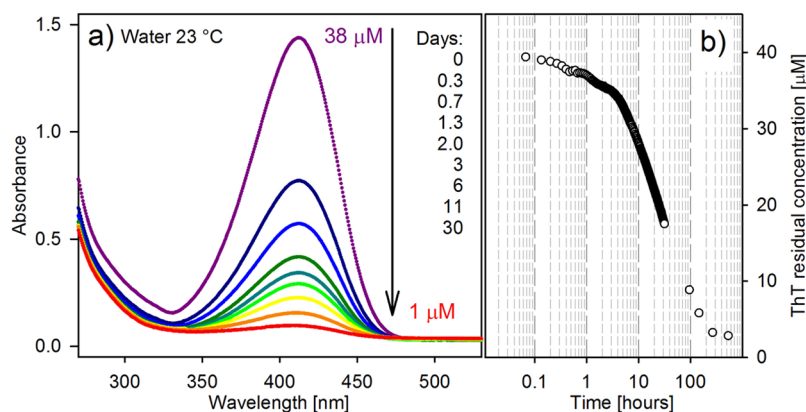


Figure 3. (a) OA spectra of residual ThT solution during an uptake in a xerogel sample. (b) Corresponding ThT residual concentration as a function of time.

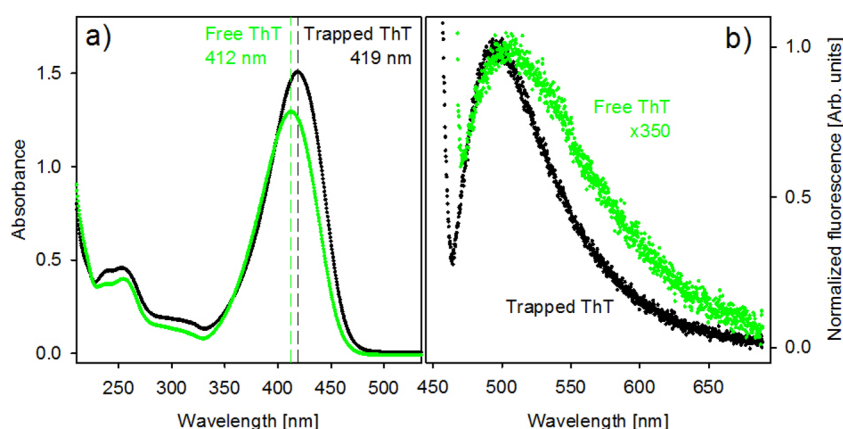


Figure 4. (a) Absorption and (b) fluorescence spectra excited at 450 nm of an aqueous solution of free ThT (green) and ThT molecules trapped inside a xerogel silica glass (black). The peak at 450 nm in panel b is the elastic Rayleigh scattering signal. The fluorescence spectrum of free ThT is multiplied by a factor of 350.

growth of the fluorescence band centered at 495 nm observed during the uptake kinetics at 36 °C could be ascribed to ThT molecules that penetrate inside the xerogel porous matrix.

Figure 2b shows the time evolution of the fluorescence intensity signal at 495 nm for three identical xerogels loaded in 40 μM ThT aqueous solution at different temperatures (23, 36, and 48 °C). Although different in absolute intensity, when normalized at 20 h, the signals superimpose, showing that at all of the investigated temperatures, the same temporal law of growth is maintained. In the observed temperature range, this result is compatible with the idea that the uptake process is not due to simple diffusion inside the matrix but it is possible to infer the existence of a preferential interaction between ThT solution and the pore surfaces of the material. Figure 2c shows the fluorescence increase at 495 nm and 23 °C as a function of the square root of the time. The purple line is the corresponding linear best fit and indicates a square root behavior of the fluorescence data at least up to 9 h of uptake.

In Figure 3a, the optical absorption (OA) spectra of the ThT aqueous solution in the uptake experiment (initial concentration of 40 μM) are shown as a function of time (in this experiment, the xerogel sample is dipped into the solution to avoid any interference with the optical path). The obtained absorption spectra show that the residual concentration of free ThT (OA band peaked at 412 nm) decrease from ~ 40 to ~ 1 μM in 1 month (see also Figure 3b). Interestingly, when the

ThT-loaded xerogel sample is dipped into a new fresh ThT solution (40 μM) a very similar kinetics is obtained (data not shown), and also in this second step, the free ThT molecules in the solution are quite totally removed and absorbed by the xerogel in 1 month.

Figure 4 shows the comparison between (panel a) OA and (panel b) fluorescence spectra of free (green) and xerogel-trapped (black) (the OA spectrum of the empty xerogel was correctly subtracted) ThT molecules. Some spectral differences in the position of absorption bands are observed, in particular, a ~ 7 nm red shift of the peak of trapped ThT molecules, analogous to the red-shifted band of ThT molecules blocked in a nanoconfined water pool³⁰ or ThT bound to insulin fibrils.^{29,31} Differences in the ultraviolet (UV) region of the OA spectrum are similar to the differences already observed for hydroxylated ThT.³² Moreover, a shape change in the corresponding fluorescence bands together with a blue shift is observed. These results indicate a specific interaction between the silica glass and the fluorophore.^{20–22,29,33}

Qualitative information on two-dimensional diffusion of dye molecules in the host matrix was obtained with the fluorescence recovery after photobleaching (FRAP) measurement by confocal microscopy,^{34–37} a technique widely used to characterize sol–gel matrices by means of diffusion of fluorescent dyes.³⁵ Figure 5 shows the time evolution of the mean fluorescence intensity I/I_0 measured at 490 nm and averaged in the red circle

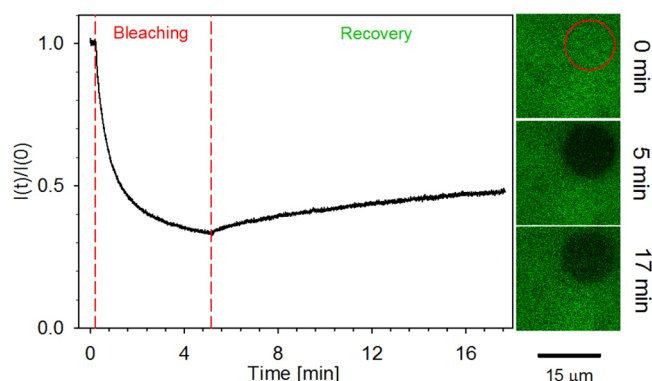


Figure 5. Fluorescence intensity as a function of time and mediated inside the red circle (diameter of 12 μm) shown in the first confocal image on the right. The images represent the laser-excited fluorescence of the sample at three moments (0, 5, and 17 min). The black bar indicates the dimensional scale.

(diameter of 12 μm) displayed in the first image on the right. The reference value I_0 is measured in a circle of the same radius, in a portion shifted with respect to the bleaching zone. As shown in Figure 5, at the end of the first step, a great part (about 65%) of the ThT molecules was bleached. In the second recovery step, the fluorescence slowly grows up and only $\sim 20\%$ of the bleached intensity was recovered, suggesting a large immobile fraction (about 80%) of molecules. Moreover, the temporal fluorescence recovery is slower than typical diffusion times of similar dyes in mesoporous matrices.^{35–37} These results indicate that, at the microscopic level, two populations of ThT molecules are present: most of ThT molecules are trapped inside the matrix, and the remaining molecules are able to slowly diffuse.

To provide evidence of the possible role of electrostatic interactions in the trapping mechanism, we performed two different experiments: (1) An uptake experiment using 2-[4-(dimethylamino)phenyl]-benzothiazole (BTA-2), an uncharged analogue of ThT (see the chemical structure represented in Figure 7), was performed. This dye shows similar features to ThT fluorescence properties: very low intensity in aqueous solutions, increase of the quantum yield after binding to amyloid fibrils, and distinct absorption and emission features in the free and bound states.^{38,39} At variance with ThT, BTA-2 is not charged, and for this reason, it was proposed as an ideal probe of amyloidosis *in vivo*, because it is able to cross the

blood–brain barrier.³⁹ Note that, in this experiment, only the properties of the fluorescent dye are varied, while the hosting matrix remains unchanged. (2) A ThT uptake experiment using a water/HCl mixture at pH 3 was performed. Indeed, at acidic pH, the number of negatively charged $\equiv\text{SiO}^-$ groups on the surface of the matrix pores (see the discussion below) is expected to be substantially reduced.^{17,40,41} Note that, in this experiment, the fluorescent dye remains unaltered, while the properties of the matrix and the solvent are changed.

Figure 6a shows the fluorescence spectra at 23 $^\circ\text{C}$ of a xerogel glass in a BTA-2 aqueous solution at the beginning of the uptake process (black) and after 30 h (blue). The weak band centered at ~ 450 nm observed at $t = 0$ is due to the BTA-2 solution surrounding the xerogel.³⁹ After loading for 30 h, the band peak position is blue-shifted and the fluorescence intensity is slightly increased, in good agreement with fibril-bound BTA-2 fluorescence.³⁹ As evident in Figure 6a, it is possible to select a spectral region where the signal of the bound dye can be singled out (dark pink shadowed area). The corresponding mean intensity as a function of time is reported in Figure 6b and clearly shows that the signal arising from uploaded BTA-2 raises with time. This result indicates that part of the BTA-2 molecules in the solution penetrates inside the matrix and that the fluorescence band of these uploaded molecules is modified by interactions with the matrix.

In Figure 7a, the comparison between the increasing fluorescence signals of ThT (black) and BTA-2 (red) is reported. Both fluorescence signals are due to dyes progressively loaded into two aged xerogel samples in an aqueous solution at the same initial concentration and temperature (the two signals were weighted at the peak of the corresponding fluorescence band and normalized for the different absorptions at corresponding excitation wavelengths and for corresponding counts of exciting lamp). As seen, the increase of the fluorescence signal is almost 1 order of magnitude smaller in the BTA-2 sample with respect to the ThT sample; notwithstanding, the increase in the quantum yield for BTA-2 in fibrillation experiments was found to be greater by a factor of 2 with respect to the corresponding increase in ThT.³⁹ This indicates a much weaker dye–matrix interaction in the case of BTA-2. However, the square root time dependence is maintained for BTA-2, as shown by the normalized data reported in the inset. In Figure 7b, the residual concentration of BTA-2 is superimposed with analogous data for ThT (see Figure 3b) as a function of the

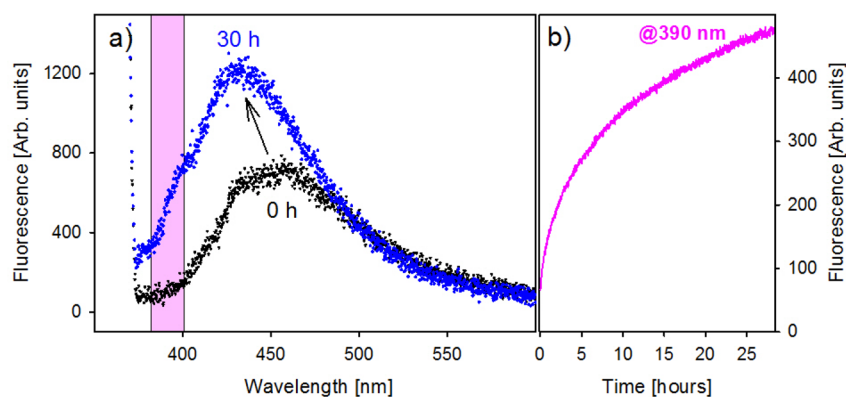


Figure 6. (a) BTA-2 fluorescence spectra (excited at 360 nm) at the beginning of the xerogel uptake (black) and after 30 h (blue). (b) BTA-2 fluorescence signal (weighted in the dark pink zone centered at 390 nm, as indicated in panel a) as a function of time at 23 $^\circ\text{C}$.

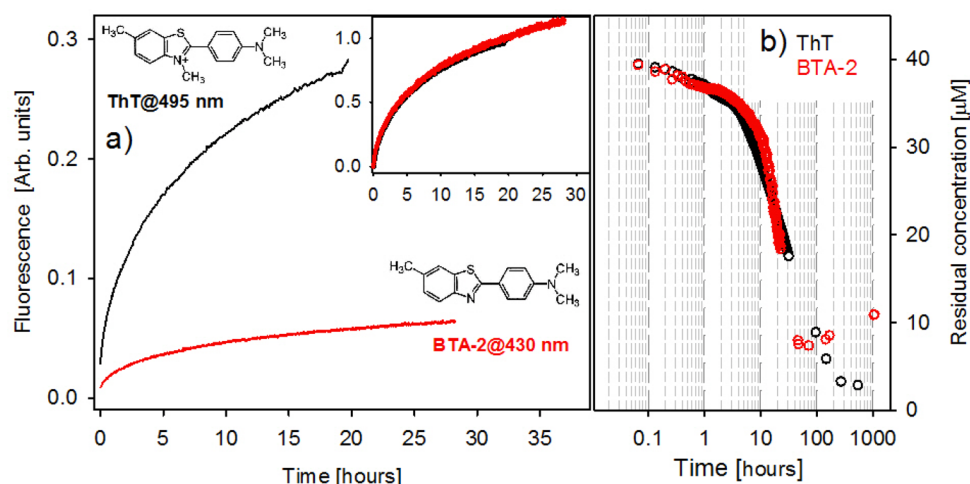


Figure 7. (a) Fluorescence signals of ThT at 495 nm (black) and BTA-2 at 430 nm (red) as a function of time at 23 °C. In the inset are shown the same data normalized at 20 h. (b) Residual concentrations for ThT (black) and BTA-2 (red) as a function of the loading time in a xerogel sample.

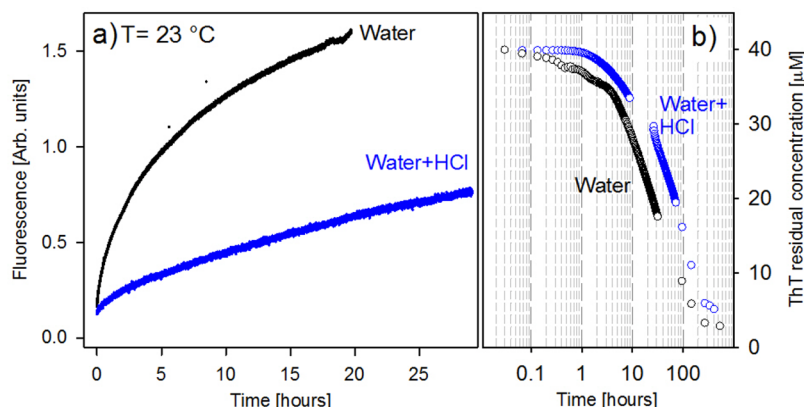


Figure 8. (a) ThT fluorescence intensity at 495 nm as a function of time for two xerogel samples loaded at 23 °C in water (black) and water + HCl (blue). (b) Free ThT absorption intensity at 412 nm as a function of time for the ThT solution with two xerogel samples dipped at 23 °C in water (black) and water + HCl (blue).

loading time. It should be noted that the residual concentration after ~24 h is very similar for both ThT and BTA-2 (and thus the dye concentrations inside the matrix). However, after 1 month, the ThT concentration tends to zero, whereas the BTA-2 concentration remains almost constant to the value of ~10 μM. From the ratio of the BTA-2 concentrations inside and outside the matrix, using the formula $\Delta E = RT \ln([BTA]_{\text{inside}}/[BTA]_{\text{outside}})$, it is possible to estimate the BTA-2 binding energy that results to be on the order of 14 kJ/mol, which is compatible with hydrogen-bonding and/or van der Waals interactions {the $[BTA]_{\text{outside}} = 10 \mu\text{M}$ was experimentally measured, as shown in Figure 6b; the $[BTA]_{\text{inside}}$ was estimated from the difference between initial and final BTA concentrations (30 μM) in solution, the mass of the xerogel (0.25 g), the total volume of the xerogel (0.15 mL), the normal silica density (2.2 g/mL), and the total volume of the BTA solution (3 mL)}. An analogous estimate for the ThT binding energy is not possible because the final ThT concentration outside the matrix is too low to be measured.

A comparison of the fluorescence signal time dependence for the samples at neutral (black) and acidic (blue) pH is reported in Figure 8a; it is evident that the fluorescence value reached after 20 h is considerably less at acidic than at neutral pH. However, if the above fluorescence signals are normalized to

the ThT concentrations inside the matrix (either estimated from the residual ThT concentration in solution or directly measured with OA), very similar values are obtained, indicating that the fluorescence quantum yield of bound ThT is almost equal at the two pH values. Data relative to the residual ThT concentration in solution are reported in Figure 8b. The trends of both curves are similar, and in particular, the residual ThT concentration tends to very low values at long times; however, the ThT decrease in the acidic solution is sizably slower.

A ThT leaching experiment was also performed as a function of pH. Five identical ThT-loaded xerogel samples were prepared and placed in a series of HCl solutions (without ThT) prepared with different pH values (1.4, 2.5, 4.0, and 5.5) and in pure water. After 3 days of dipping, the presence in solution of ThT molecules (released by the xerogels) was measured by absorption spectroscopy. Figure 9 shows the concentration of leached ThT molecules as a function of pH.

Frequency-domain lifetime measurements were performed to estimate the fluorescence quantum yield of ThT molecules trapped in a xerogel sample.⁴² In Figure 10 is shown the result of a measurement on the ThT xerogel sample: phase delays (black left axis) and modulation ratios (red right axis) are plotted as a function of the modulation frequency of the exciting light. The continuous lines are the best fit of the

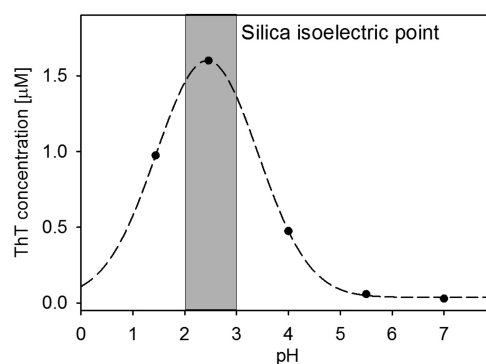


Figure 9. Concentration of leached ThT molecules as a function of pH. The dashed line is a Gaussian fit of the data only with eye-guide purposes.

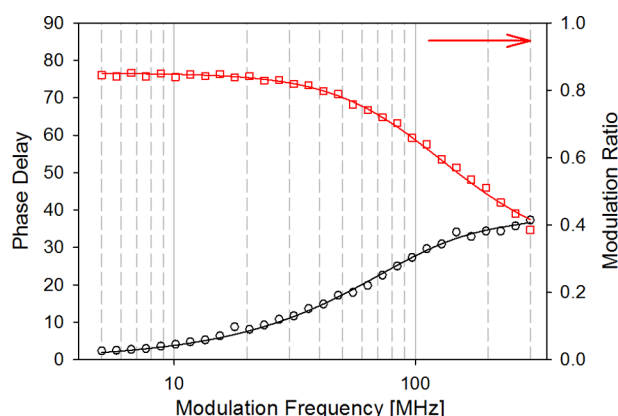


Figure 10. (Black left axis) Phase delay and (red right axis) modulation ratio as a function of the modulation frequency of the exciting light for the ThT xerogel sample. The continuous lines are the best fit of experimental data to a double exponential decay.

experimental data to a double exponential decay for estimating the lifetime inherent in the fluorescence signal.⁴² The results on the found lifetimes τ_i and their weights f_i for the samples loaded with ThT are reported in Table 1 together with the mean lifetime calculated with the expression $\tau_m = \sum f_i \tau_i$, with the condition $\sum f_i = 1$.

The xerogel samples used in this work have been prepared by the sol–gel technique,^{15,43} and previous studies have demonstrated that, in analogous chemical conditions of the sol, the final xerogels show an high degree of porosity with a mean pore dimension in the range of 1–10 nm.^{8,12,14,44} It was observed that the size of the pores is crucial for the ability of the silica to absorb water, with pores in the range of 1–10 nm giving good hydrophilic materials.^{8,14} However, the hydrophilic character of the matrix is also dependent upon the presence of silanol groups ($\equiv\text{SiOH}$) decorating the surface of the pores.^{45,46} Indeed, the interaction between these groups and water molecules by hydrogen bonding regulates the physical properties of the porous surface of the xerogel and confined water.^{45,46}

Our silica xerogels are able to irreversibly trap a great number of ThT molecules. In fact, when a silica xerogel is dipped into a $\sim 40 \mu\text{M}$ ThT solution, not only the ThT concentration in solution tends to zero in about 1 month but, if the ThT-loaded xerogel is dipped into a fresh ThT solution also in this second step, the ThT molecules are quite totally removed from the solution being absorbed in the xerogel.

The main experimental evidences could be summarized as follows: (1) The fluorescence of ThT absorbed in the xerogel presents a very high intensity with respect to ThT aqueous solution (see Figure 2a). (2) The loading kinetics of ThT are irreversible, and in the temperature interval of ~ 20 – 50°C , they obey a square root trend, at least in the first 9 h (see panels b and c of Figure 2). (3) After 1 month, the final ThT residual concentration is practically zero, indicating that the uptake process is not a simple diffusion process driven by a concentration gradient (see Figure 3b). (4) The absorption and fluorescence bands of ThT inside the xerogel are different from corresponding spectra of free ThT molecules (see panels a and b of Figure 4). (5) The fluorescent ThT molecules inside the porous matrix are quite immobile. However, a smaller fraction of ThT molecules able to diffuse is also observed (see Figure 5). (6) The uptake kinetics of BTA-2 molecules (the uncharged analogue of ThT) shows the same temporal trend as ThT (see Figure 7a). However, a much lower fluorescence increase is observed, and at variance with ThT, the residual concentration of free BTA-2 molecules in solution reaches an equilibrium value of $\sim 10 \mu\text{M}$ after ~ 1 month (see Figure 7b). (7) At acidic pH, the ThT-loading kinetics is largely slower than at neutral pH; this notwithstanding the fluorescence intensity of trapped ThT molecules is very similar (see Figure 8). (8) Previously trapped ThT molecules leach out from the xerogel at pH near the isoelectric point of silica (see Figure 9).

These results suggest the following molecular description: ThT molecules penetrate in the nanoporous matrix of the xerogel with a diffusive process likely influenced by nano-capillary forces [moreover, it was observed that the ThT-loading kinetics depends upon the initial hydration degree of the xerogel samples (data not shown)]; while diffusing, they statistically find stable binding locations (wells), which are capable of immobilizing (or confining) them, counting them out from the diffusion process. As result, the bound molecule presents a different OA band and an enhanced fluorescence, as previously obtained for ThT in amyloid fibrils²⁹ and other confining matrices.¹⁸ We suggest that, for the positively charged ThT molecules, electrostatic interactions are the main interactions responsible for this effect. Indeed, it is well-known that the sol–gel technique produces xerogel with a higher concentration of H_2O molecules and OH groups with respect to other silica glass preparation techniques.^{11,47} The OH groups, in particular, terminate some of the silicon atoms of the inner pore surfaces forming the silanol groups, $\equiv\text{SiOH}$.^{11,47} These groups could be responsible for electrostatic binding of positive ThT molecules. Indeed, in the presence of liquid water, the following reaction:



Table 1. Best Fitting Parameters Obtained for the Investigated Xerogel Sample and Relative Errors

	τ_1 (ns)	f_1 (%)	τ_2 (ns)	f_2 (%)	τ_m (ns)
ThT-loaded xerogel	1.73 ± 0.10	65 ± 4	0.22 ± 0.06	35 ± 4	1.20 ± 0.16

is shifted to the right, leaving a negative charge on the walls of the pores.^{17,40,41} These negative charges could bind the positive ThT molecules, as was found for positive rhodamine 6G molecules trapped inside silica glass.¹⁷ The ThT⁺–SiO[−] interaction is very strong (i.e., the ThT binding wells are very deep), and this gives to the xerogel its extraordinary efficiency in sequestering the ThT molecules from the solution. The number of OH groups per unit surface area in silica is a constant value (4.9×10^{18} OH/m²),⁴⁸ and using a reasonable value for the specific surface in our samples (250 m²/g),^{8,12} we estimated a ThT saturation value (hypothesizing a 1:1 link between OH and ThT) of $\sim 2 \times 10^{-3}$ mol/g. This value is 4000 times greater than the amount of ThT inserted into the glass in one cycle ($\sim 5 \times 10^{-7}$ mol/g). Thus, the number of ThT binding sites is huge with respect to the number of ThT molecules. Moreover, the presence of OH groups on the pore surfaces gives hydrophilicity to the material, and the absorption process is favored by nanocapillary forces that, in this nanometric system, are likely to be very strong⁴⁹ and almost independent from the temperature in the range studied here.^{45,46,50} Note that both diffusion and capillarity give a square root time dependence,^{49,51} as experimentally observed in our sample (see Figure 2c).

The dependence of the ThT incorporation rate (estimated from experiments, such as that in Figure 3b) in the first 3 h was also studied as a function of the initial ThT concentration in the range of 3–40 μ M. A linear dependence was found (data not shown), indicating a first-order process with a kinetic constant of $k = (7.2 \pm 0.9) \times 10^{-6}$ s^{−1}. This result confirms that one ThT molecule at a time interacts with the matrix.

These experimental observations could give interesting insight also about the ThT interaction with amyloid fibrils and, in particular, about the observed differences in fluorescence intensity when ThT is bound to different fibril morphologies,²² which could be ascribed to a specific interaction with differently charged side chains constituting the core structure of the fibril.

Results of the BTA-2 experiment are in line with the above hypothesis. Indeed, the motional freedom of the uncharged BTA-2 molecules inside the matrix pores could be restricted through either hydrogen bonding with silanol groups (and/or through van der Waals contacts) or steric hindrance in smaller pores (and/or because of increased viscosity of confined water^{45,52,53}). However, it results in a less effective immobilization with respect to ThT binding and, therefore, a much weaker fluorescence increase, as observed in Figure 7. As a consequence, the xerogel is much less effective in sequestering the BTA-2 molecules from the solution; the ratio of the inside/outside BTA-2 concentrations gives a binding free energy of only 14 kJ/mol, in agreement with the proposed role of hydrogen-bonding and van der Waals interactions. Regardless of the interaction mechanism of BTA-2 molecules, the molecular diffusion is driven by nanocapillary forces for both ThT and BTA-2 molecules and is responsible for the shape of the uptake kinetics observed. This explains why the temporal trends of fluorescence increase, depicted in the inset of Figure 7a, are the same.

In other mesoporous systems, the effect of reversible hydrogen bonding between guest molecules (Nile Red) and the matrix was already proposed to explain their reduced mobility^{54,55} and, in general, hydrophobic interactions were excluded because of their weak nature.¹⁷

The proposed mechanism also accounts for the ThT uptake experiment performed at pH 3. In this case, less $\equiv\text{SiO}^-$ groups are present on the pore surface (see eq 1) and the ThT molecules diffusing inside the matrix find fewer binding wells. Therefore, at a given time, fewer ThT molecules are bound and the uptake process is slower. However, the binding still involves the strong ThT⁺–SiO[−] electrostatic interaction. This explains the facts that the normalized fluorescence intensities of bound ThT molecules are almost equal at the two pH values and that the residual ThT concentration in solution at acidic pH tends to zero (although at longer times). However, the two kinetics cannot be superimposed, indicating two different temporal processes. This can be explained considering that the driving nanocapillary forces mainly depend upon pore dimension but also the presence of OH groups at the surface.⁴⁵ In acidic conditions, the number of $\equiv\text{Si}-\text{O}^-$ groups is likely to be less with respect to water. Thus, the two kinetics are not superimposable at variance with the comparison between ThT and BTA-2 (same matrix and same pH).

The electrostatic binding model is also confirmed by the leaching experiment results shown in Figure 9. Indeed, at neutral pH, the ThT molecules are steadily trapped in the silica matrix. Near the isoelectric point of silica (pH 2–3), the probability of an exchange between a ThT molecule and a proton in a $\equiv\text{SiO}^-$ binding site is very high and the ThT molecules could leach out from the silica. At very acidic pH, the great number of positive protons in the local environment is likely to slow the detachment of a positive ThT molecule, so that after 3 days, a smaller ThT concentration is found in solution.

The results on the fluorescence lifetime of ThT molecules incorporated in the xerogel glass (see Figure 10) are in very good agreement with the above conclusions. Indeed, two lifetimes are observed in agreement with FRAP results. Moreover, using a radiative lifetime value of 8.0 ns for ThT (mean value calculated from refs 30 and 31), the quantum yield results $q = 0.15 \pm 0.02$, which is 1500 times greater than the corresponding q for free ThT molecules.³¹ This strongly confirms our model, indicating that the xerogel glass environment around the ThT molecules efficiently hinders the rotational modes of the molecule.

CONCLUSION

The results of this paper indicate that amorphous mesoporous silica xerogels can be used to irreversibly trap dye molecules. In the case of ThT, a xerogel of ~ 0.15 mL immersed in 3 mL of ~ 40 μ M ThT solution is able to effectively remove almost all dye molecules from the solution in a couple of weeks. The resulting material is a highly fluorescent xerogel in an almost “clean” solution.

We identify the main physical origin of this trapping effect, i.e., the electrostatic interaction between the positively charged ThT molecule and the negatively charged $\equiv\text{SiO}^-$ groups decorating the inner surface of the matrix pores. This interaction strongly hinders the rotational mobility of the dye, increasing its fluorescence quantum yield 1500 times and changing the absorption and fluorescence bands of ThT, as observed in other confining media.

We also show that suitable alteration of the electrostatic effect (by varying the charge on the dye molecule and/or the matrix) enables us to fine tune the extent and time course of the dye uptake and the release of the trapped dye molecules. These results therefore constitute a preliminary but essential

step toward the production of materials with controlled fluorescence features and/or with “solution cleaning” properties.

■ EXPERIMENTAL SECTION

A solution containing 75% (v/v) tetramethyl orthosilicate (Merck), 20% H₂O (Millipore purified, resistivity of $\sim 18 \text{ M}\Omega \text{ cm}$), and 5% HCl ($2 \times 10^{-3} \text{ M}$) is sonicated for $\sim 20 \text{ min}$ and diluted with an equal quantity of water (final pH 2). After gentle mixing, the resulting sol is poured into semi-micro polystyrene cuvettes (Kartell, 1 cm path length). In these conditions, gelification of the sample occurs in about 1 h at room temperature following two main processes: a hydrolysis and a condensation phase.^{1,9,11–13} In the first phase, the metal alkoxides interact with water to produce alcohol and the $\equiv\text{SiOH}$ groups. In the second phase, the interaction of $\equiv\text{SiOH}$ groups with themselves (water condensation) or with the metal alkoxides (alcohol condensation) produces a gel network by cross-linking between silicon and oxygen atoms with the release of water or more alcohol, respectively. This network constitutes the skeleton of small particles, which, in a further polymerization process, condenses together, forming the overall glass matrix. After a few days, this “wet” hydrogel sample can be extracted from the cuvette. If the wet silica hydrogel is left to age at room temperature, it progressively loses weight and reduces its volume until it reaches, after about 15 days, approximately one-seventh of its initial volume. The final dimensions of the slab are about $1.3 \times 0.5 \times 0.24 \text{ cm}^3$. No further relevant volume contraction is observed upon prolonged aging, although the structure of the matrix and the water content of the hydrogels keep evolving, as shown by the near-infrared (NIR) absorption spectrum.⁴³ The data reported in this paper refer mainly to a dry xerogel that was left to age at room temperature for about 24 months. The hydration, $h = \text{grams of } [\text{H}_2\text{O}]/\text{grams of } [\text{SiO}_2]$, was about 30%.

ThT (T3516) was purchased from Sigma Aldrich (the counterion is a Cl atom) and purified using the recrystallization protocol described elsewhere.²⁵ The molar extinction coefficient of $36\,000 \text{ M}^{-1} \text{ cm}^{-1}$ was used to obtain the ThT concentrations.²¹ BTA-2 (88302) was purchased from Anaspec and used as obtained. Both dyes were prepared at a final molar concentration of $40 \mu\text{M}$ in aqueous solution. Fluorescence measurements were performed in a standard right-angle geometry on a $1.0 \times 1.0 \text{ cm}$ PMMA UV cuvette (BRAND) filled with the dye solution, with an homemade positioning system for the dipped xerogel sample.

The glass samples were mounted in back scattering at 45° with respect to the excitation light. The excitation light produced by a xenon lamp (75 W) was set at 450 nm for ThT (360 nm for BTA-2) with a first spectrograph (SpectraPro 2150i, PI Acton, 150 mm focal length) equipped by a 150 grooves/mm grating blazed at 500 nm (at 300 nm for BTA-2). The fluorescence produced by the sample was dispersed by another spectrograph (SpectraPro 2300i, PI Acton, 300 mm focal length) equipped by a 300 grooves/mm grating (blazed at 500 nm, emission bandwidth of 10 nm) and was detected by an air-cooled (-80°C), intensified 1340×400 charge coupled device (PIXIS 400BR, PI Acton). The temporal window for acquiring the fluorescence light was set to be 1 ms for ThT and 5 ms for BTA-2, and different spectra were acquired to obtain a data pitch of 60 s in uptake experiments. The weak fluorescence of free ThT molecules in solution was acquired with a higher integration time of 1 s. Because of the long time measurements of several hours, care was taken to ensure that variation in lamp efficiency did not affect the experimental data; part of the excitation light was reflected by a beam splitter mirror toward an auxiliary detector, whose signal was used to normalize the sample fluorescence. It has to be noted that, in all measurements, the ThT fluorescence is not affected by the hydroxylation process, which could invalidate the analysis of fluorescence kinetics.³²

For the FRAP measurement, a ThT-loaded xerogel sample was placed on a microscope slide and imaged using a Leica RCS SP5 confocal laser scanning microscope with a $63\times$ oil objective numerical aperture (NA) = 1.4 (Leica Microsystems, Germany). The confocal

experiment was performed using the available FRAP wizard of the LEICA control software.

OA measurements on xerogels before and after the ThT uptake were performed on a double-monochromator JASCO V-560 spectrophotometer.

Frequency domain lifetime measurements were performed on a ISS-K2 phase and modulation fluorimeter with a vertical polarized diode excitation (436 nm) and a photomultiplier tube (PMT) detection of polarized (54.7°) fluorescence light after a band-pass filter ($485 \pm 15 \text{ nm}$) to reject most of the scattered exciting light. A glycogen solution was used as a reference sample, and measurements were performed varying the modulation frequency between 2 and 300 MHz in a logarithmic scale. To verify the validity of the frequency-domain lifetime setup, a xerogel glass was impregnated in a diluted aqueous rhodamin B (RhB) solution. RhB is a fluorescent molecule widely used for its constant quantum yield (~ 0.3 in aqueous solution) independent from the excitation energy.^{42,56} After 24 h of impregnation, the xerogel sample became reddish according to the incorporation of the RhB molecules. In our measurement, the fluorescence of trapped RhB molecules decays with a single lifetime of $2.45 \pm 0.10 \text{ ns}$ (data not shown). This value is in good agreement with the lifetime of 2.40 ns recently found for RhB molecules incorporated in a modified mesoporous silica.⁵⁷

■ AUTHOR INFORMATION

Corresponding Author

*E-mail: michele.damico@unipa.it

Present Address

†Institut de Biologie Structurale, Centre National de la Recherche Scientifique (CNRS), 38027 Grenoble, France.

Notes

The authors declare no competing financial interest.

■ ACKNOWLEDGMENTS

This work was partly financially supported by a national project (PRIN 2008) of the Italian Ministry of University and Research. The authors thank the other members of the MBSM group (<http://www.fisica.unipa.it/biophysmol/>), Dr. Gianpiero Buscarino (Dipartimento di Fisica e Chimica, Università degli Studi di Palermo), Dr. Sergio Giuffrida (Dipartimento di Fisica e Chimica, Università degli Studi di Palermo), and Dr. Vito Foderà (Department of Drug Design and Pharmacology, University of Copenhagen) for very useful discussions. The recrystallized ThT was kindly provided by Dr. Minna Groenning (Department of Pharmacy, University of Copenhagen). The authors thank Prof. G. Chirico and Prof. M. Collini (Department of Physics, Milano-Bicocca University) for the frequency domain lifetime measurement.

■ REFERENCES

- (1) Reisfeld, R. *J. Fluoresc.* **2002**, *12*, 317–325.
- (2) Davis, M. E. *Nature* **2002**, *417*, 813–821.
- (3) Sanchez, C.; Julian, B.; Belleville, P.; Popall, M. *J. Mater. Chem.* **2005**, *15*, 3559–3592.
- (4) Avnir, D.; Coradin, T.; Lev, O.; Livage, J. *J. Mater. Chem.* **2006**, *16*, 1013–1030.
- (5) Trewyn, B. G.; Giri, S.; Slowing, I. I.; Lin, V. S. Y. *Chem. Commun.* **2007**, 3236–3245.
- (6) Chen, Z.; Jiang, Y.; Dunphy, D. R.; Adams, D. P.; Hodges, C.; Liu, N.; Zhang, N.; Xomeritakis, G.; Jin, X.; Aluru, N. R.; Gaik, S. J.; Hillhouse, H. W.; Brinker, C. J. *Nat. Mater.* **2010**, *9*, 667–675.
- (7) Moerz, S. T.; Knorr, K.; Huber, P. *Phys. Rev. B: Condens. Matter Mater. Phys.* **2012**, *85*, 075403.
- (8) Yariv, E.; Reisfeld, R.; Saraidarov, T.; Axelrod, E.; Rysakiewicz-Pasek, E.; Wodnicka, K. *J. Non-Cryst. Solids* **2002**, *305*, 354–361.
- (9) Dunn, B.; Zink, J. I. *Acc. Chem. Res.* **2007**, *40*, 747–755.

- (10) Hutter, T.; Amdursky, N.; Gepshtein, R.; Elliott, S. R.; Huppert, D. *Langmuir* **2011**, *27*, 7587–7594.
- (11) Brinker, C. J.; Scherer, G. W. *Sol–Gel Science: The Physics and Chemistry of Sol–Gel Processing*; Academic Press: Waltham, MA, 1990.
- (12) Curran, M. D.; Stiegman, A. J. *Non-Cryst. Solids* **1999**, *249*, 62–68.
- (13) Gupta, R.; Chaudhury, N. *Biosens. Bioelectron.* **2007**, *22*, 2387–2399.
- (14) Fidalgo, A.; Ilharco, L. M. *Chem.—Eur. J.* **2004**, *10*, 392–398.
- (15) Cammarata, M.; Levantino, M.; Cupane, A.; Longo, A.; Martorana, A.; Bruni, F. *Eur. Phys. J. E: Soft Matter Biol. Phys.* **2003**, *12*, 63–66.
- (16) Santangelo, M. G.; Levantino, M.; Vitrano, E.; Cupane, A. *Biophys. Chem.* **2003**, *103*, 67–75.
- (17) Ye, F.; Collinson, M. M.; Higgins, D. A. *Phys. Chem. Chem. Phys.* **2009**, *11*, 66–82.
- (18) Amdursky, N.; Erez, Y.; Huppert, D. *Acc. Chem. Res.* **2012**, *45*, 1548–1557.
- (19) Selkoe, D. J. *Nature* **2003**, *426*, 900–904.
- (20) Langkilde, A. E.; Vestergaard, B. *FEBS Lett.* **2009**, *583*, 2600–2609.
- (21) Groenning, M. J. *Chem. Biol.* **2010**, *3*, 1–18.
- (22) Biancalana, M.; Shohei, K. *Biochim. Biophys. Acta* **2010**, *1804*, 1405–1412.
- (23) Doerr, A. *Nat. Methods* **2011**, *8*, 376–378.
- (24) Alavez, S.; Vantipalli, M. C.; Zucker, D. J. S.; Klang, I. M.; Lithgow, G. J. *Nature* **2011**, *472*, 226–229.
- (25) D'Amico, M.; Di Carlo, M. G.; Groenning, M.; Militello, V.; Vetri, V.; Leone, M. J. *Phys. Chem. Lett.* **2012**, *3*, 1596–1601.
- (26) Stsiapura, V. I.; Maskevich, A. A.; Kuzmitsky, V. A.; Uversky, V. N.; Kuznetsova, I. M.; Turoverov, K. K. *J. Phys. Chem. B* **2008**, *112*, 15893–15902.
- (27) Stsiapura, V. I.; Maskevich, A. A.; Tikhomirov, S. A.; Buganov, O. V. *J. Phys. Chem. A* **2010**, *114*, 8345–8350.
- (28) Singh, P.; Kumbhakar, M.; Pal, H.; Nath, S. J. *Phys. Chem. B* **2010**, *114*, 2541–2546.
- (29) Sulatskaya, A. I.; Kuznetsova, I. M.; Turoverov, K. K. *J. Phys. Chem. B* **2012**, *116*, 2538–2544.
- (30) Singh, P. K.; Kumbhakar, M.; Pal, H.; Nath, S. J. *Phys. Chem. B* **2009**, *113*, 8532–8538.
- (31) Sulatskaya, A. I.; Maskevich, A. A.; Kuznetsova, I. M.; Uversky, V. N.; Turoverov, K. K. *PLoS One* **2010**, *5*, No. e15385.
- (32) Foderà, V.; Groenning, M.; Vetri, V.; Librizzi, F.; Spagnolo, S.; Cornett, C.; Olsen, L.; van de Weert, M.; Leone, M. J. *Phys. Chem. B* **2008**, *112*, 15174–15181.
- (33) LeVine, H., III. *Methods Enzymol.* **1999**, *309*, 274–284.
- (34) Meyvis, T.; De Smedt, S.; Van Oostveldt, P.; Demeester, J. *Pharm. Res.* **1999**, *16*, 1153–1162.
- (35) Weiss, A. M.; Saraidarov, T.; Reisfeld, R. *Opt. Mater.* **2001**, *16*, 15–20.
- (36) Hellriegel, C.; Kirstein, J.; Bräuchle, C.; Latour, V.; Pigot, T.; Olivier, R.; Lacombe, S.; Brown, R.; Guieu, V.; Payraastre, C.; Izquierdo, A.; Mocho, P. J. *Phys. Chem. B* **2004**, *108*, 14699–14709.
- (37) Hungerford, G.; Rei, A.; Ferreira, M. I. C.; Tregidgo, C.; Suhling, K. *Photochem. Photobiol. Sci.* **2007**, *6*, 825–828.
- (38) Klunk, W. E.; Wang, Y.; Huang, G.-f.; Debnath, M. L.; Holt, D. P.; Mathis, C. A. *Life Sci.* **2001**, *69*, 1471–1484.
- (39) Kitts, C.; Vanden Bout, D. J. *Fluoresc.* **2010**, *20*, 881–889.
- (40) Lan, E. H.; Dave, B. C.; Fukuto, J. M.; Dunn, B.; Zink, J. I.; Valentine, J. S. *J. Mater. Chem.* **1999**, *9*, 45–53.
- (41) Rosenholm, J. M.; Czurylszkiewicz, T.; Kleitz, F.; Rosenholm, J. B.; Lindén, M. *Langmuir* **2007**, *23*, 4315–4323.
- (42) Lakowicz, J. R. *Principles of Fluorescence Spectroscopy*, 3rd ed.; Springer: New York, 2006.
- (43) Cupane, A.; Levantino, M.; Santangelo, M. G. *J. Phys. Chem. B* **2002**, *106*, 11323–11328.
- (44) Fidalgo, A.; Rosa, M. E.; Ilharco, L. M. *Chem. Mater.* **2003**, *15*, 2186–2192.
- (45) Takei, T.; Mukasa, K.; Kofuji, M.; Fuji, M.; Watanabe, T.; Chikazawa, M.; Kanazawa, T. *Colloid Polym. Sci.* **2000**, *278*, 475–480.
- (46) Fekkar-Nemmiche, N.; Devautour-Vinot, S.; Coasne, B.; Henn, F.; Mehdi, A.; Reye, C.; Corriu, R.; Collet, A. *Eur. Phys. J.: Spec. Top.* **2007**, *141*, 45–48.
- (47) Vella, E.; Boscaino, R.; Navarra, G. *Phys. Rev. B: Condens. Matter Mater. Phys.* **2008**, *77*, 165203.
- (48) Zhuravlev, L. *Colloids Surf., A* **2000**, *173*, 1–38.
- (49) Gruener, S.; Sadjadi, Z.; Hermes, H. E.; Kityk, A. V.; Knorr, K.; Egelhaaf, S. U.; Rieger, H.; Huber, P. *Proc. Natl. Acad. Sci. U.S.A.* **2012**, *109*, 10245–10250.
- (50) Crupi, F.; Longo, F.; Majolino, D.; Venuti, V. *Eur. Phys. J.: Spec. Top.* **2007**, *141*, 61–64.
- (51) Huber, P.; Grüner, S.; Schäfer, C.; Knorr, K.; Kityk, A. V. *Eur. Phys. J.: Spec. Top.* **2007**, *141*, 101–105.
- (52) Santangelo, M. G.; Levantino, M.; Cupane, A.; Jeschke, G. J. *Phys. Chem. B* **2008**, *112*, 15546–15553.
- (53) Xu, S.; Scherer, G. W.; Mahadevan, T. S.; Garofalini, S. H. *Langmuir* **2009**, *25*, 5076–5083.
- (54) Fu, Y.; Ye, F.; Sanders, W. G.; Collinson, M. M.; Higgins, D. A. *J. Phys. Chem. B* **2006**, *110*, 9164–9170.
- (55) Ye, F.; Higgins, D. A.; Collinson, M. M. *J. Phys. Chem. C* **2007**, *111*, 6772–6780.
- (56) Magde, D.; Rojas, G. E.; Seybold, P. G. *Photochem. Photobiol.* **1999**, *70*, 737–744.
- (57) Yamaguchi, A.; Namekawa, M.; Itoh, T.; Teramae, N. *Anal. Sci.* **2012**, *28*, 1065–1070.